DEVELOPMENTS IN NUCLEAR SPECTROSCOPY

A Thesis

Submitted in partial fulfilment of

the requirements for the degree of

Master of Science

at

University of Manitoba

by

G. Isford

April, 1951.

PREFACE.

The work to be described in the following pages was carried out at the University of Manitoba during 1950-51 as part of a project of "Investigation of Nuclear Energy Levels" being conducted by Dr. R. W. Pringle.

TABLE OF CONTENTS

P A R T A

P A R T B.

PART A

INVESTIGATIONS

OF

A LARGE AREA

SEMI-PERMANENT MAGNET

FOR USE IN A BETA SPECTROMETER

INTRODUCTION

In the many experiments where it is necessary to use magnetic fields for deflecting particles, it is often essential that the magnetic field remain constant to at least one part in a thousand. An ideal way of attaining this constancy is by use of a semi-permanent magnet in place of the more usual electromagnet or Helmholtz coil arrangement. We thus avoid the complication of maintaining extremely large and stable currents over long periods of time.

The first such magnet to be made specifically for beta ray spectroscopy was designed by J. D. Cockroft, C. D. Ellis, and H. Kershaw at Cambridge.(1) It consisted of a soft iron yoke with poles of 35% Cobalt steel. Three coils were disposed on each pole, and pole pieces were of soft iron 17 cm. by 29 cm. with an air gap of 5.5 cm. having a field of 2000 oersteds. This enabled particles with an $H\rho$ (Field strength X radius of curvature of beta particles) of 24,000 oersted cm. to be focussed within a 2 per cent uniform field.

The magnet at present under investigation is an improvement on this design inasmuch as the poles are of Alcomax II, a new high permeability magnet alloy.

---

(1) J. D. Cockroft, C. D. Ellis, H. Kershaw .. A Permanent Magnet for Beta Ray Spectroscopy, Proc. of Royal Soc. Vol.135 P.628 (1932)

In use, the former magnet focussed particles of different energy at different radii of curvature onto a photographic plate. The gap field strength, once set, was not altered. However, in the magnet being investigated it is desired to focus particles of different energies at a given radius of curvature by varying the field in the gap. Hence the purpose of this investigation is first to check the uniformity of the field in the gap to determine the maximum radius of curvature lying entirely within a one per cent uniform field, and secondly to determine the best operating procedure with the magnet in order to cover the required H range in extremely small increments. The latter requires the design of a field control panel and an accurate field measuring device.

DESCRIPTION OF THE MAGNET

With the Cockroft & Ellis cobalt steel magnet as a guide, and with the following design changes made by Dr. R. W. Pringle, the magnet was cast by Wm. Jessop and Sons Ltd., Sheffield. An increase in the pole face area to 26 cm. by 39 cm. was made, thus providing a larger possible radius of curvature and hence better resolution of beta particle energies. Decreasing the gap field strength to 1200 oersteds still retained the magnet's ability to focus particles of momentum 20,000 oersted-cms. and an increase in the gap width to 6.5 cms. facilitated working in the gap. Further, through use of the new alloy Alcomax II, the weight of the magnet was cut down to less than one third, and the overall dimensions to less than one half of the cobalt steel magnet (which weighed 2400 pounds, and was 133 cms. long).

Figure I illustrates the assembly for the new magnet. The yoke is made of Armco Iron 57.5 cm. long, 36.0 cm. high and has a cross sectional area of 20 cms. by 7 cms. The poles of the magnet each consist of six blocks of Alcomax II magnet alloy 5.5 cm. by 9.5 cm. by 14.2 cms., drilled through the centre and bolted from the yoke to the pole pieces. The pole pieces are 26 cm. by 39 cm. and 4.5 cm. thick, tapered back to the alcomax blocks and supported by brass uprights as shown. The coils, wound on brass frames each fit over the alcomax II poles and consist of 1440 turns of 16 s.w.g. cotton covered copper wire capable

of carrying a steady current of seven amps.

The magnet is shown in Figure II mounted on a cement supporting block in its present working position.

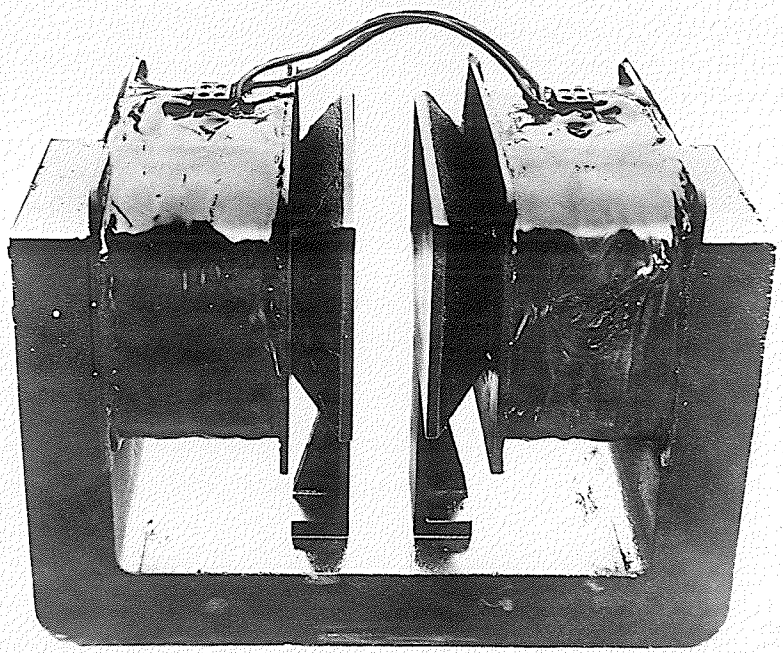

FIG. I

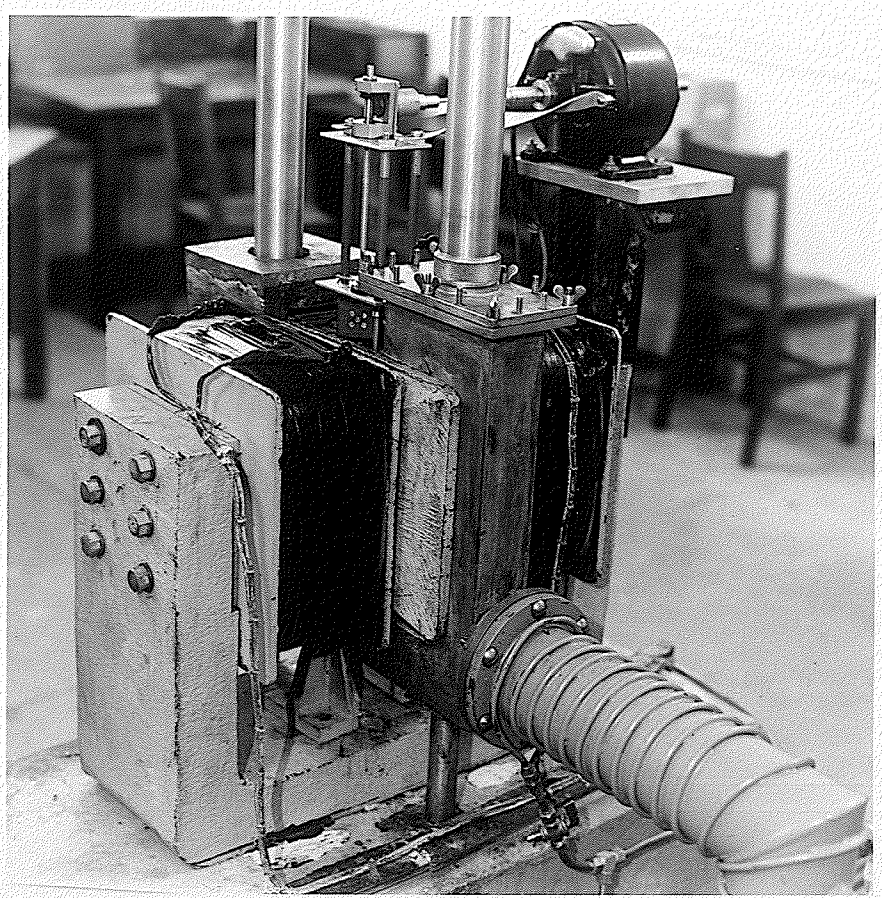

FIG. II

THE B. H. CURVE.

Before considering the special properties of the magnet alloy Alcomax II it will facilitate the discussion to consider some of the properties of magnetic materials in general.

The BH curve, or hysteresis loop, is typical of almost all magnetic materials. It is obtained from measurements on a specimen in a closed loop without air gaps. Figure III illustrates the normal form of this curve. The principal points marked are the remanence (B_R) point, the maximum energy (BH_{max}) point, and the coercive (H_C) point. If at any point such as P, the steady cyclic change in H is reversed in direction, then the flux density changes along an internal curve such as PR. If from R, the field H retraces its values, the flux density traverses the upper half of the loop PR until it again reaches P, after which the main curve will be followed. Such a minor loop is known as a recoil loop.

In a permanent magnet system in which there is an air gap, magnetic flux threads the gap, and hence magnetic energy exists in the air gap. This energy has come from the permanent magnet, which must be self de-magnetized to the extent necessary to provide this energy. If H_S is the magnetic field in the steel of length l_S, and H_g is the field strength in the air gap of length l_g, then when no magnetizing force due to currents is present, the sum of the

magnetomotive forces around the magnetic circuit gives

$$\int H_s \, dl_s + \int H_g \, dl_g = 0$$

Hence if the field (H_g) is positive, the field strength (H_s) inside the magnet must be negative. This means that a magnetic system with an air gap must work in the upper left hand quadrant of the hysteresis loop in Figure III.

MAGNETIC PROPERTIES OF ALCOMAX II.

The magnet alloy Alcomax II is a Ni-Al-Fe alloy whose exact composition has not yet been revealed. However, it has the special property of being anisotropic. It has been found[1] that cooling a ferromagnetic substance through the Curie point, and through the temperature range in which plastic flow occurs, the magnetostrictive strains are to some extent relieved, and the actual direction of magnetization of each domain becomes an energetically favored direction of magnetization. These directions would normally be at random through the material as a whole, but if a field is applied during cooling they will be so distributed so as to favor subsequent bulk magnetization parallel to the original applied field. Then for this particular axis of the material, the remanent magnetization is approximately equal to the saturated magnetization. The properties of exceptionally high remanence, high coercivity and very high energy value are thus confined principally along the preferred axis. The disparity of these properties along the preferred and the axis perpendicular to the preferred are shown in Figure IV which represents the upper left hand quadrant of the saturation

---

(1) D. A. Oliver, J. W. Shedden, Nature Vol.132 P.209 (1938).

Hysteresis loop.[1] Average properties along the preferred axis are:-

Remanence	-	12,400 gauss
Coercive Force	-	570 oersted
$(BH)_{max}$	-	4,300,000 (at B = 9600 H = 450)

These properties can be compared with 35 percent Cobalt Steel used in the Cockroft and Ellis permanent magnet.

Remanence	-	9000 gauss
Coercive Force	-	250 oersted
$(BH)_{max}$	-	950,000 (at B = 5,950 H = 160)

Since a magnet, demagnetized by the air gap alone, must work at values of B and H corresponding to a point on the demagnetization quadrant of the main hysteresis loop, it can be readily seen how such a large volume saving was effected in the Alcomax II magnet without loss in performance.

This Alcomax II material has also an exceptional degree of magnetic stability and can be artificially aged to stabilize it for all normal usage. Since it also retains its basic magnetic properties unchanged at temperatures up

---

(1) Permanent Magnet Alloys, Booklet published by Permanent Magnet Association, 301 Glossop Road, Sheffield.

to 550° C, the magnet will be unaffected by normal temperature variations.

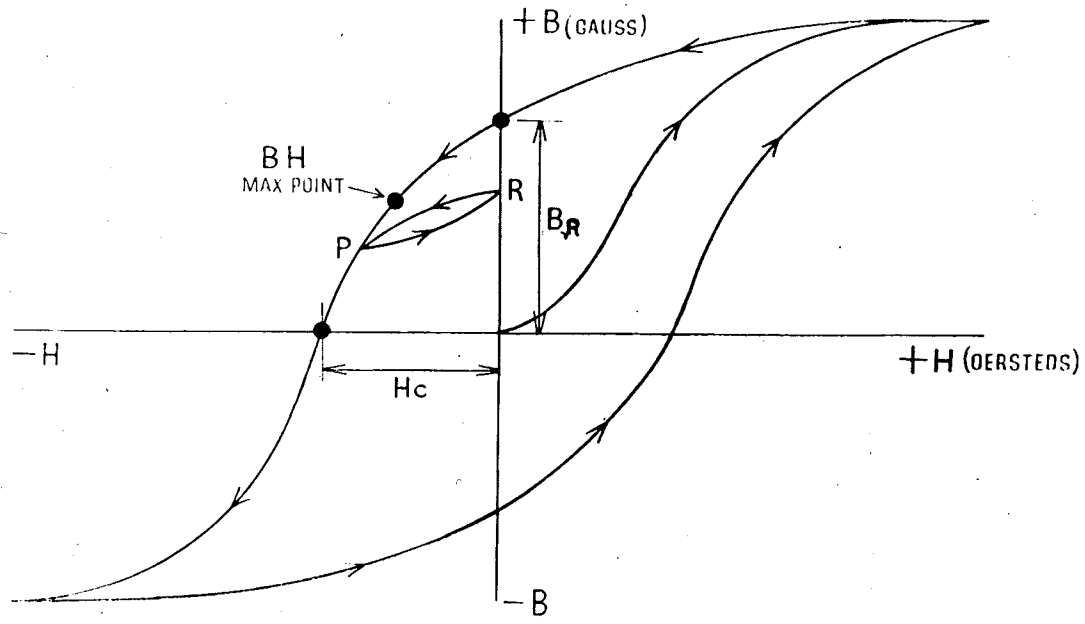

FIG. III

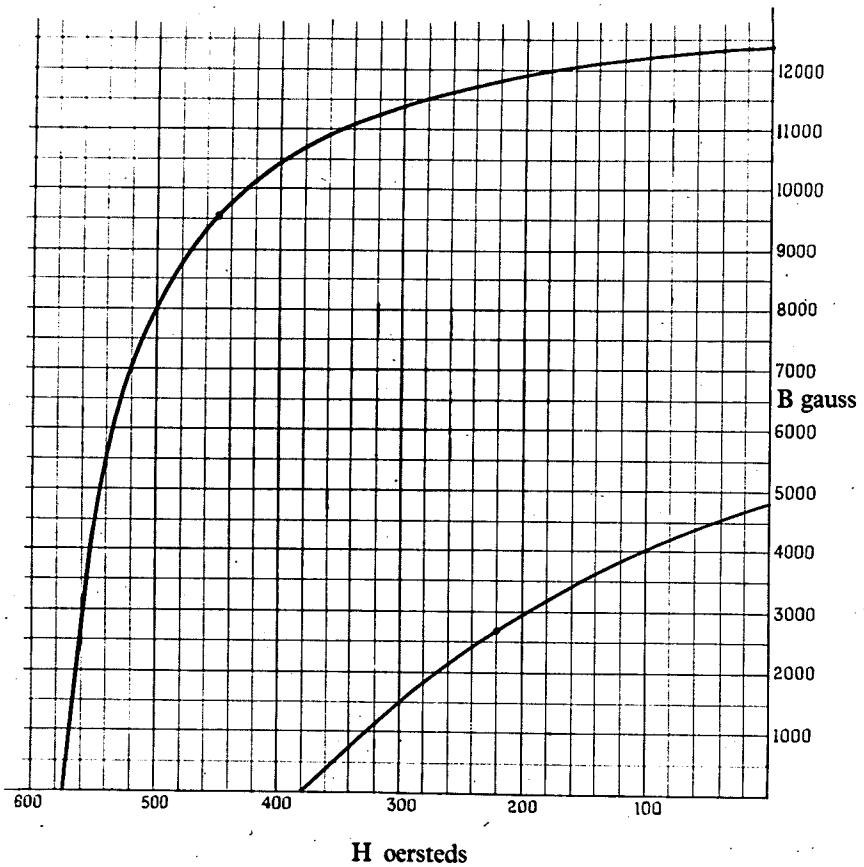

FIG. IV

UNIFORMITY OF FIELD

THE COIL

To determine the area over which the field was uniform to within one percent, it was necessary to first design a flip coil whose axis could be fixed into any required position in the air gap. The design decided upon is shown in Figure X. The coil consisted of two wraps of number 20 B & S copper wire, totaling ninety seven turns, with an effective area of 293.4 square cms. Stops were located on the frame so that turning of the knob rotated the coil through exactly 180°. When used in conjunction with a Rawson fluxmeter, also shown in Figure X, this gave a deflection of one division corresponding to a field of 34.1 gauss, so that the saturation field of 1200 oersted corresponded to 37 divisions, or almost the full scale deflection. It was found possible with practice to read deflections to within one tenth of a division, or .3% accuracy. To move the coil from point to point within the gap, the movable side could be released by the off centre screw cams and then re-tightened in the new position quite rapidly.

FIELD UNIFORMITY INVESTIGATIONS

With the magnet at its saturation point, the pole face was divided into a cartesian co-ordinate grid system with one cm. between points. The flip coil was then located at

each point in turn, and the average of several "flips" taken as the field strength at the point. In critical regions, additional points were taken to establish continuity, and all results were plotted in the form of a contour pattern on the face of the N pole.

The first contour corresponds to a fall off of one half of one percent from the centre peak value of approximately 1260 oersteds, as illustrated in Figure VI. The fact that the central contour encloses a slightly higher field in the lower central right hand region is probably due to the fact that the gap is a little narrower in this region, due to a slight lack of uniformity in the pole surfaces combined with a lack of complete parallelism in the surfaces. Although gap measurements were attemped with a micrometer no measurable difference could be found.

It will be noted how the field gradient increases very rapidly towards the edges of the pole pieces. The two percent contour corresponds on the top and both sides with the taper on the back of the pole piece, but not along the bottom. This lower region would seem to have a greater tendency to field uniformity than the top. The one percent contour is within two cms. of the bottom, whereas it is 3.5 cms. from the top. This may be due to the lines of induction having a greater tendency to fringe on top, rather than within the yoke at the bottom.

From the area within the one percent contour it is found that the radius of curvature for beta particles must

be limited to 16 cms., and the focussing must be carried out on an area 3.5 cms. in from the top and sides of the pole piece.

SPECIAL FIELD INVESTIGATIONS.

When the magnet is in operation, the vacuum box in which the beta particles are focussed, occupies the air gap. Hence to determine the field at all times it is necessary to locate a measuring device in the fringing field at the top of the gap.

An investigation of this fringing field was made with the "flip coil" described on page 10, but in this case the handle was held vertically as the coil was raised to positions above the gap. Field determinations were made up the centre line of the air gap and the results appear in Figure V. Although the field gradient appears almost linear in the short distance of interest above the gap, it "tails" off less rapidly with distance "d" for readings further up from the gap. When the field was changed to a point on a recoil loop by passing 5.25 amps in the reverse direction for a few seconds, the same proportionality between fringing field and central field was maintained within the experimental error.

Since the flip coil averages the flux in an area of almost three square cms., it was thought advisable to make a miniature flip coil with an area less than one $cm.^2$ to investigate any special field effects that might occur

around four small pits in the surface of the pole piece face. This coil when wound had a volume of approximately one cubic cm. and a thousand turns of # 40 B & S Copper wire. Used in conjunction with the same Rawson fluxmeter, no significant field variation could be detected. This miniature coil, because of its high resistance, could not be used easily for absolute field determinations.

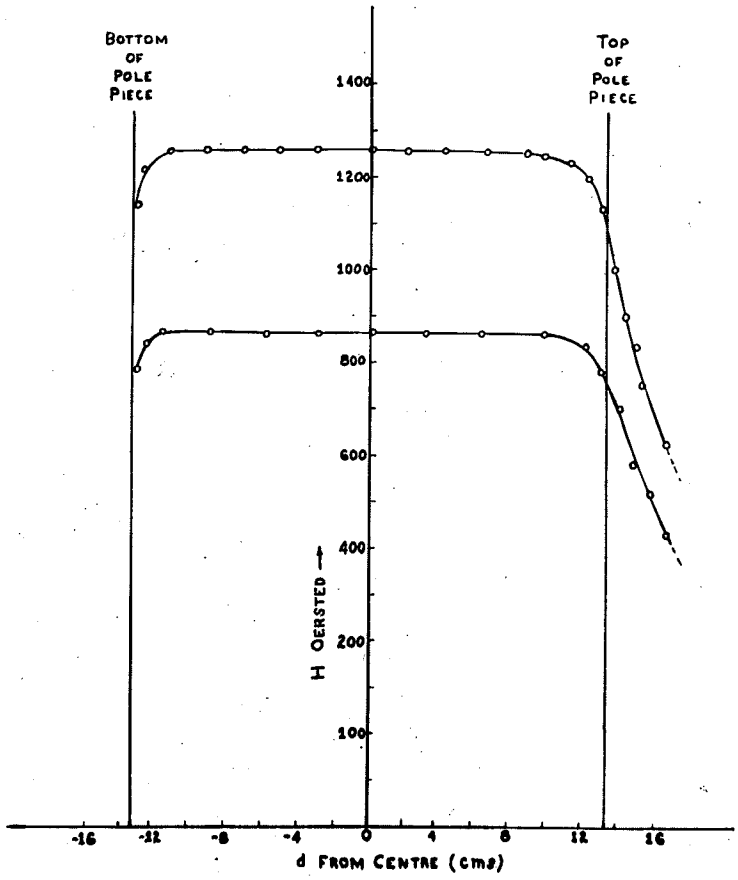
Bottom of Pole Piece
Top of Pole Piece
1400
1200
1000
800
600
400
200
100
H Oersted
-16
-12
-8
-4
0
4
8
12
16
d From Centre (cms)

Fig V

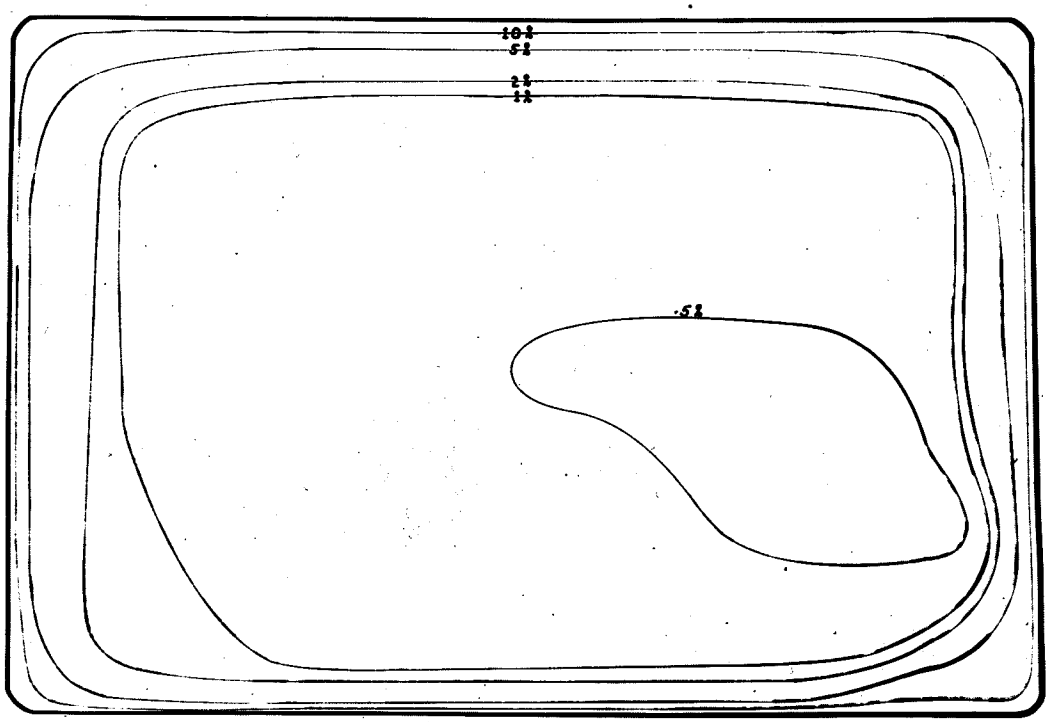
10%
5%
2%
1%
.5%

Fig VI

FIELD CONTROL INVESTIGATIONS.

CONTROL PANEL

As full control of the magnetic field requires extremely heavy currents from the 220 volt D.C. generator as well as finely controlled currents up to 11 amps. from a 120 volt lead cell bank, it was necessary to combine these D.C. sources into a special field control panel for both safety and facility of control.

A photograph of the completed panel appears in Figure VII and a schematic wiring diagram in Figure VIII. In use, the voltage selector is thrown to the D.C. source which is desired, the reversing switch is thrown to right or left depending on whether the field is to be reinforced or demagnetized, the appropriate mains switch is then set and the magnet input switch pushed to the "on" position. The resistance selector switch permits control of the current to any desired value. The components of this control are shown in greater detail in Figure IX.

The resistances are so arranged that continuous variation of current can be made up to eleven amperes without breaking the circuit. To facilitate reading the currents it was found necessary to include a parallel bank of three ammeters which, covering the complete current range, could be inserted or removed from the circuit with knife switches as desired, without breaking the circuit.

To accommodate the high back E.M.F. resulting when

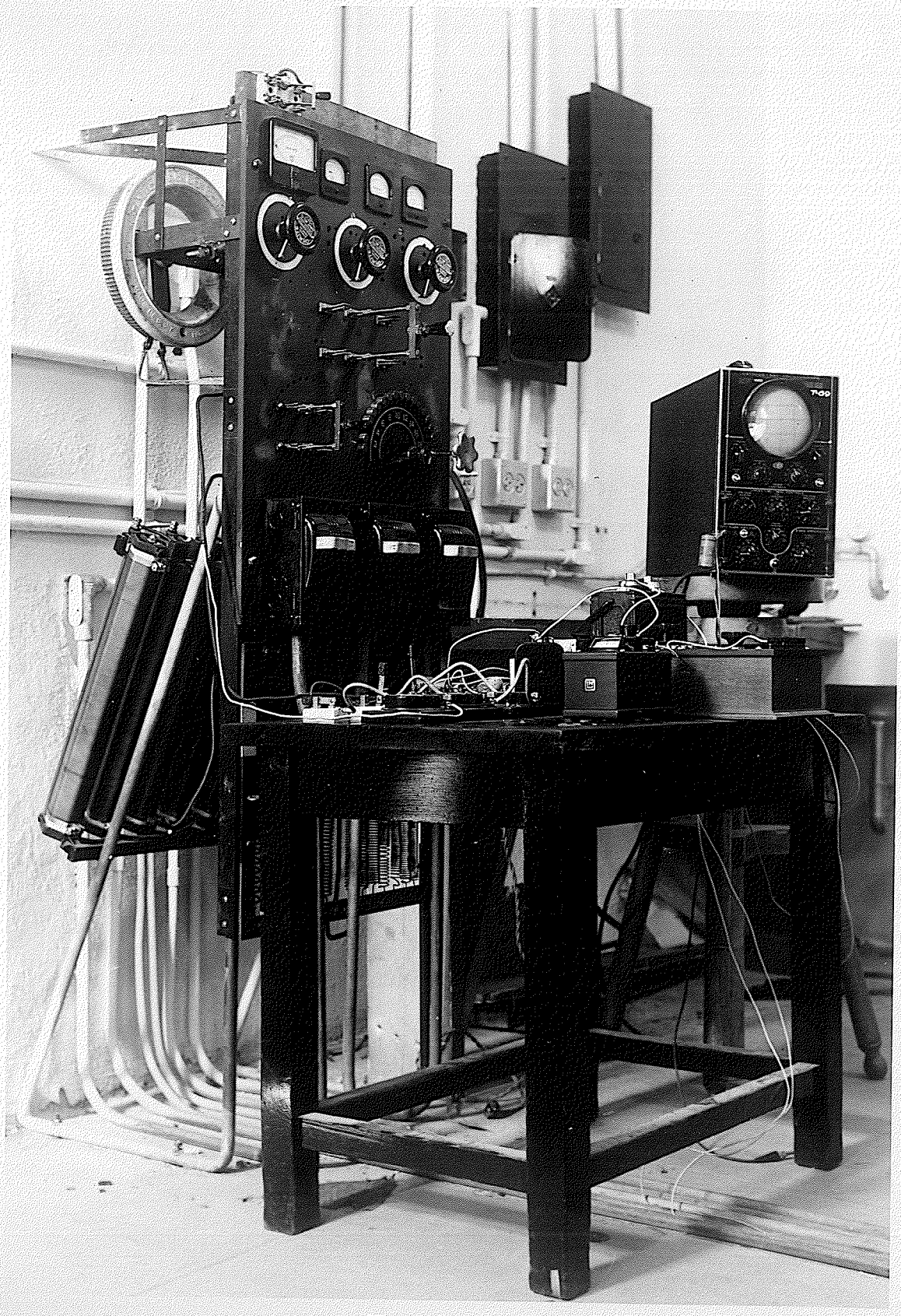

FIG VII

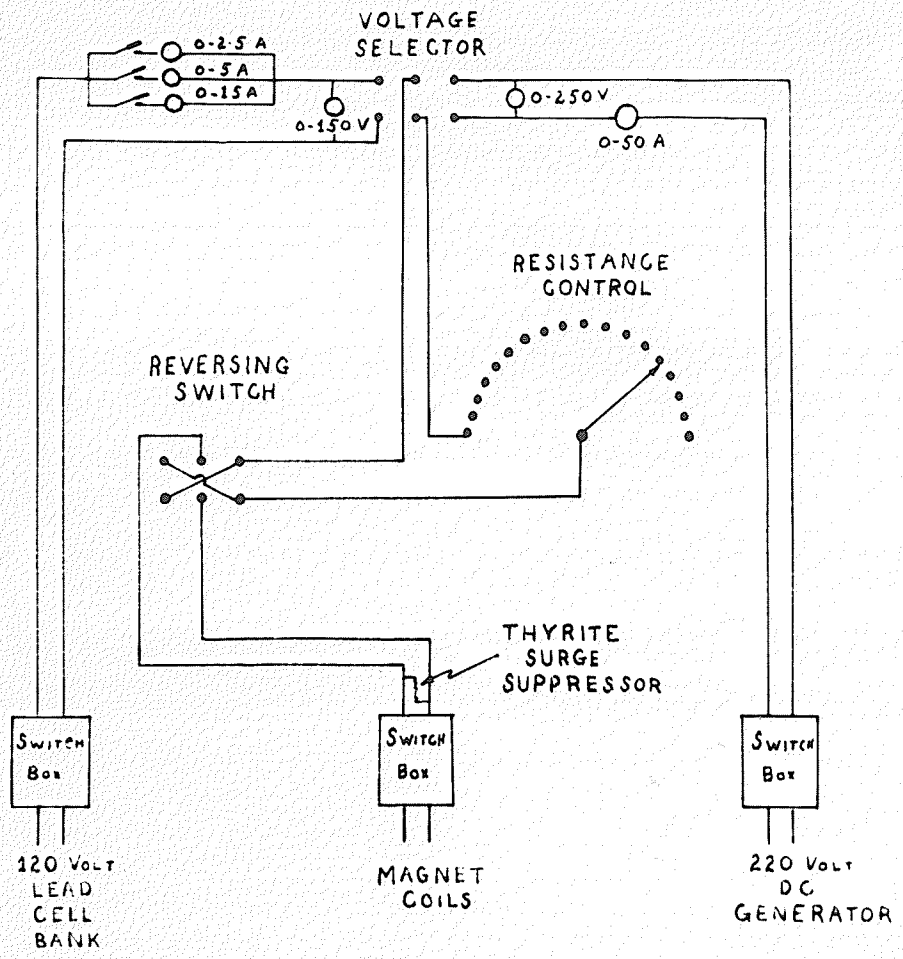

FIG VIII

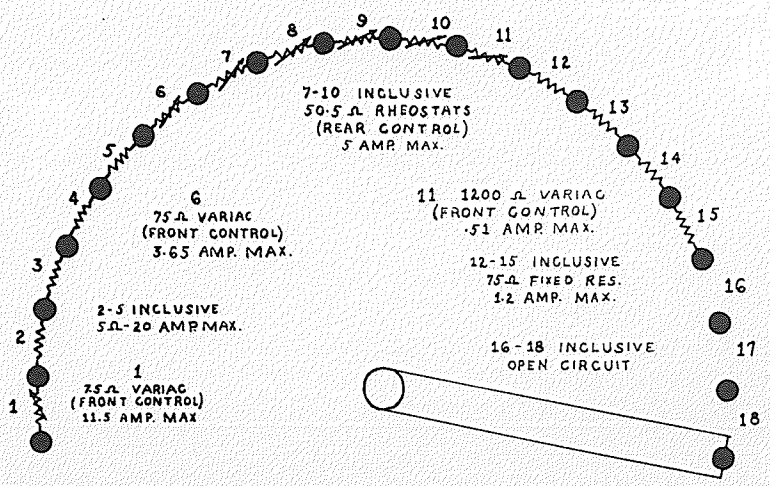

FIG IX

a saturation current is broken, a 600 volt D.C. General Electric Thyrite surge suppressor was put in parallel with the magnet input terminals. All wiring from the panel was enclosed in conduit as shown and properly fused in the switch boxes.

FIELD MEASURING DEVICE

Since it was desirable to have an accuracy in field measurements better than that obtainable with the flip coil, the following method was used.

A Synchronous motor (Westinghouse Type CSS Synchronous at 1800 r.p.m.) was geared through a one to one ratio system to rotate a coil in the fringing field at the top of the magnet. The voltage output from this coil, tapped off a split ring copper commutator with silver brass alloy brushes, was measured on a Potentiometer (Leeds and Northrup Student type). The motor and coil arrangement is shown in Figure XI, while the potentiometer assembly can be seen in the view of the field control panel Figure VII.

The shape of the output pulse from the coil is monitored at all times with a Cathode Ray Oscillograph (Allen B. Dumont Laboratories) to determine, first, whether the coil is rotating synchronously and secondly whether any commutator noise is present. With the trace frequency set to line frequency, the coil output trace pattern was locked only when the coil was rotating

synchronously at 1800 r.p.m. and this generally required a minute or two from the starting of the motor. After an hour or two it was usually found that heating could cause commutator noise distortion in the output. This could be removed by applying mineral oil to the commutator and brushes; the oscilloscope trace becoming smooth again within a few minutes.

For a coil of total effective area A. rotating in the magnetic field H with an angular velocity ω , with the E.M.F. tapped off as described, the average value of V recorded by the potentiometer is given by:

$$V = \frac{1}{\pi} \int_0^{\pi} HA\omega \sin \omega t \; d(\omega t)$$

$$= \frac{2}{\pi} HA\omega$$

$$\text{or} \quad H = \frac{\pi}{2A\omega} V = KV$$

At balance on the potentiometer no current is drawn from the coil, hence the resistance of coil and leads may be neglected. It has been shown (Figure V) that the fringing field is proportional to the central field strength H, and so this constant of proportionality may be included in K and the value of K determined by focussing a known energy beta particle such as the Au^{198} 411 kev gamma ray conversion electrons. (See P.21). The H value required to focus this line corresponds to a K of 260 units, and evaluating KV for the saturation field gives H = 1260 oersteds, in good agreement with the value obtained earlier with the flip coil data.

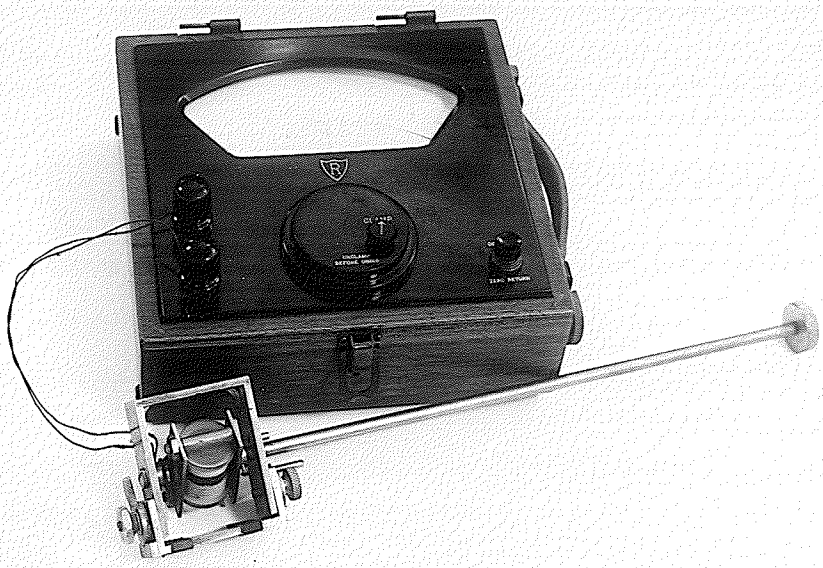

FIG. X

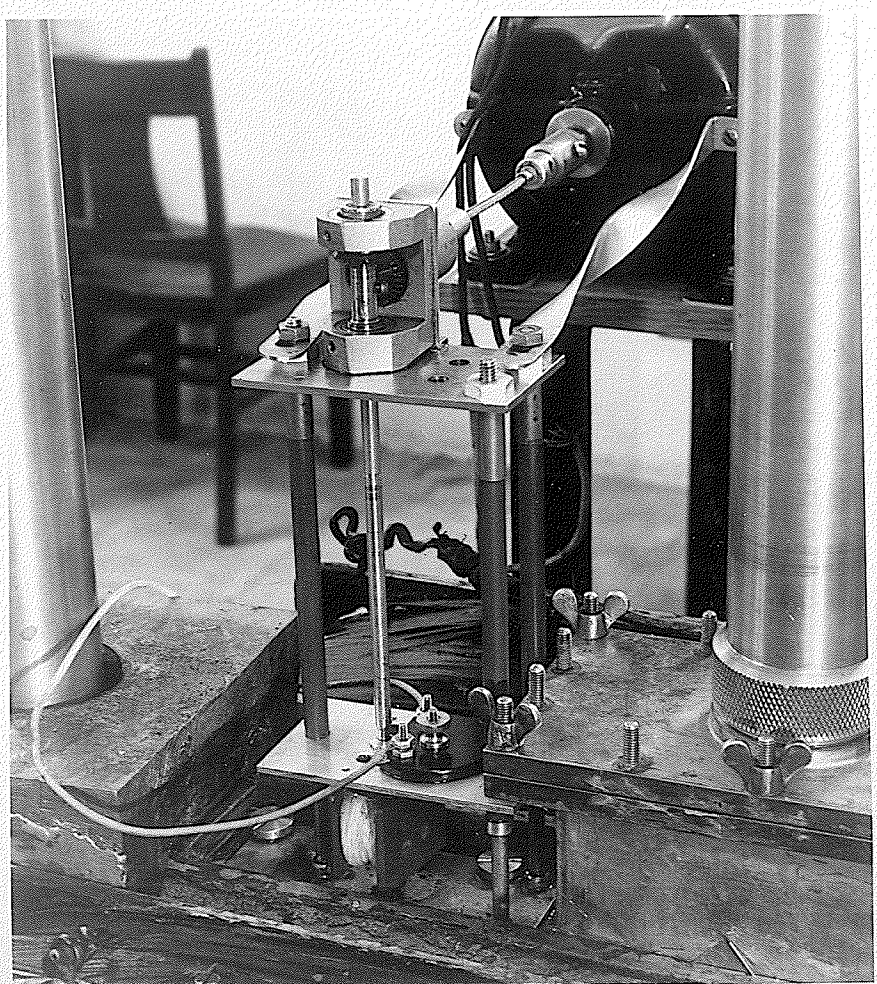

FIG. XI

For voltage readings up to 1.6 volts it was found that voltage differences of one part in fifteen hundred could be distinguished. For voltage readings above 1.6 volts, the limit of the potentiometer used, it was necessary to employ a voltage divider. The output from the coil was put across a five megohm chain of Shollcross precision wound resistances and the potential drop across one tenth of this chain was put into the potentiometer. It was necessary to use a more sensitive galvanometer ($k = 8 \times 10^{-8}$ coulombs/mm/@ 10 cm.), but the same accuracy was found to prevail with this arrangement.

SATURATION LOOP.

To saturate the magnetic field, the procedure was to set the resistance control to zero resistance and short the 220 volt generator across the magnet coils in parallel for a second or two. Since the total circuit resistance is approximately five ohms, this meant that approximately forty amperes would be drawn from the generator. This large current had to be almost instantaneous since it represents a current almost three times in excess of the rating for the coil windings. It was found that at least three such surges were required to produce peak saturation in the gap, the third surge producing an increase of less than .04 volts in 5.80. Five further surges succeeded in producing an increase of only .01 volts.

To investigate the saturation loop, a demagnetizing

current from the 120 volt lead cell bank was put through the coils. This current was steadily increased in increments of one half to one ampere without backtracking, simultaneous voltage readings being taken at each point. The results appear in Figure XII in the second and third quadrants, and it will be seen that the curve approximates the shape of the hysteresis loop of a ferromagnetic specimen without an air gap. The current range was limited to eleven amperes since this is the maximum current the resistance control unit could dissipate.

To investigate the upper range of field strengths available, the magnet was again saturated with three generator surges and a reinforcing current was then fed through the coils. Voltage readings were taken as the current was increased in half ampere increments to a maximum of ten amperes and then back to zero. This loop appears in the first quadrant of Figure XII. It will be noted that its amplitude is very small, that it is a closed loop, and that it provides a range of field strengths up to approximately 1700 oersteds.

RECOIL LOOPS.

Since it is necessary that stabilizing currents be constant over long periods, it is desirable to keep them as small as possible, and yet be able to cover the range of field strengths desired on any one run. This can be done providing the magnet working point, with zero stabilizing

current, can be preset accurately at any desired value.

To do this it was necessary to investigate the recoil loops from the main saturation loop (ABC) in Figure XIII. It was found that if a demagnetization current of a few amperes was put through the coils (taking the field strength from saturation point A to a point, say B, further down the saturation loop), then broken, the new working point (E) was somewhat below the saturation point (A). This point (E) we will call the recoil point. Rebuilding the demagnetization current returned the field to the original point (B) on the saturation curve, and increasing the current carried the field to points (CD etc.) farther down the saturation loop. The actual paths taken in going from the saturation loop to the recoil points for currents of nine amperes (CF) and ten amperes (DG) are also shown in Figure XIII, and it will be noted these are very nearly straight lines.

Recoil points for currents of several different values were determined, and it will be noted that the straight lines approximating these loops are all parallel. This property makes the problem of arriving at any desired working point rather easy. One merely draws another parallel line through the desired working point on the zero current axis (say G) and notes from the current intercept on the saturation loop (D), the necessary demagnetizing current (10 amperes) which must be applied to saturation field (A), and broken, to bring the field to this recoil point.

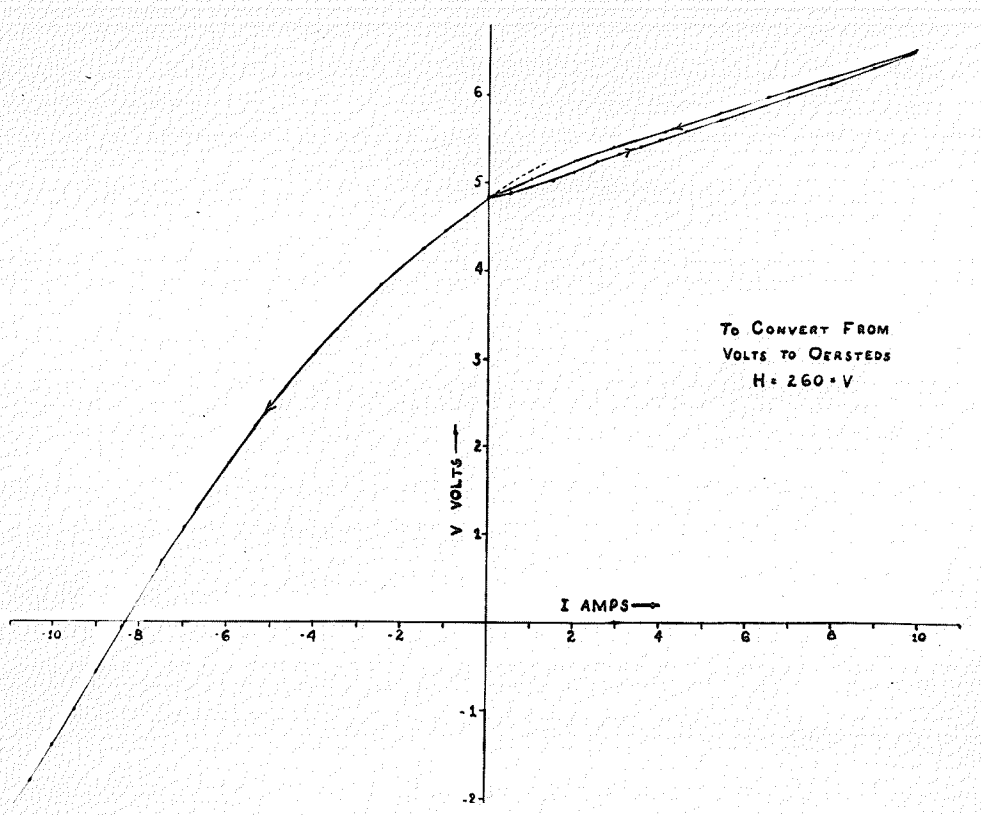

FIG. XII

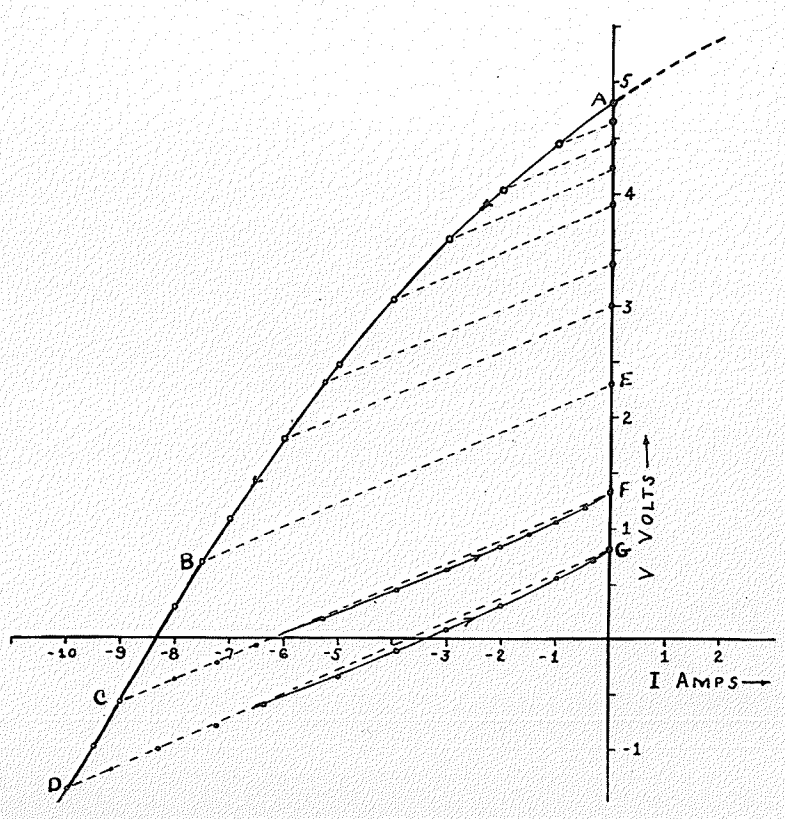

FIG. XIII

AUXILIARY LOOPS.

In operation, when reinforcing and demagnetizing currents are applied at the working point, the magnet actually works on a small auxiliary loop within the saturation loop. It was thought desirable to learn something about the shape of these inner loops.

The magnet was first brought to the ten ampere recoil point from saturation field. Ten ampere reinforcing and demagnetizing currents were then put through the coils several times to establish the loop, then voltage readings were taken as the field was taken around the cycle in small current increments. The results appear in Figure XIV. It will be noted that the loop closes exactly at A, but has a considerable thickness throughout. Backtracking with the current at C takes the field through an internal auxiliary loop, but increasing it past C again takes the field along the original loop.

Putting the field through a 3.5 ampere auxiliary loop from the ten ampere recoil point gives a loop with the same characteristic shape as the large loop, but appended to the large loop at B. It will be noted in both cases that the most linear portions of the cycle appear in the negative half.

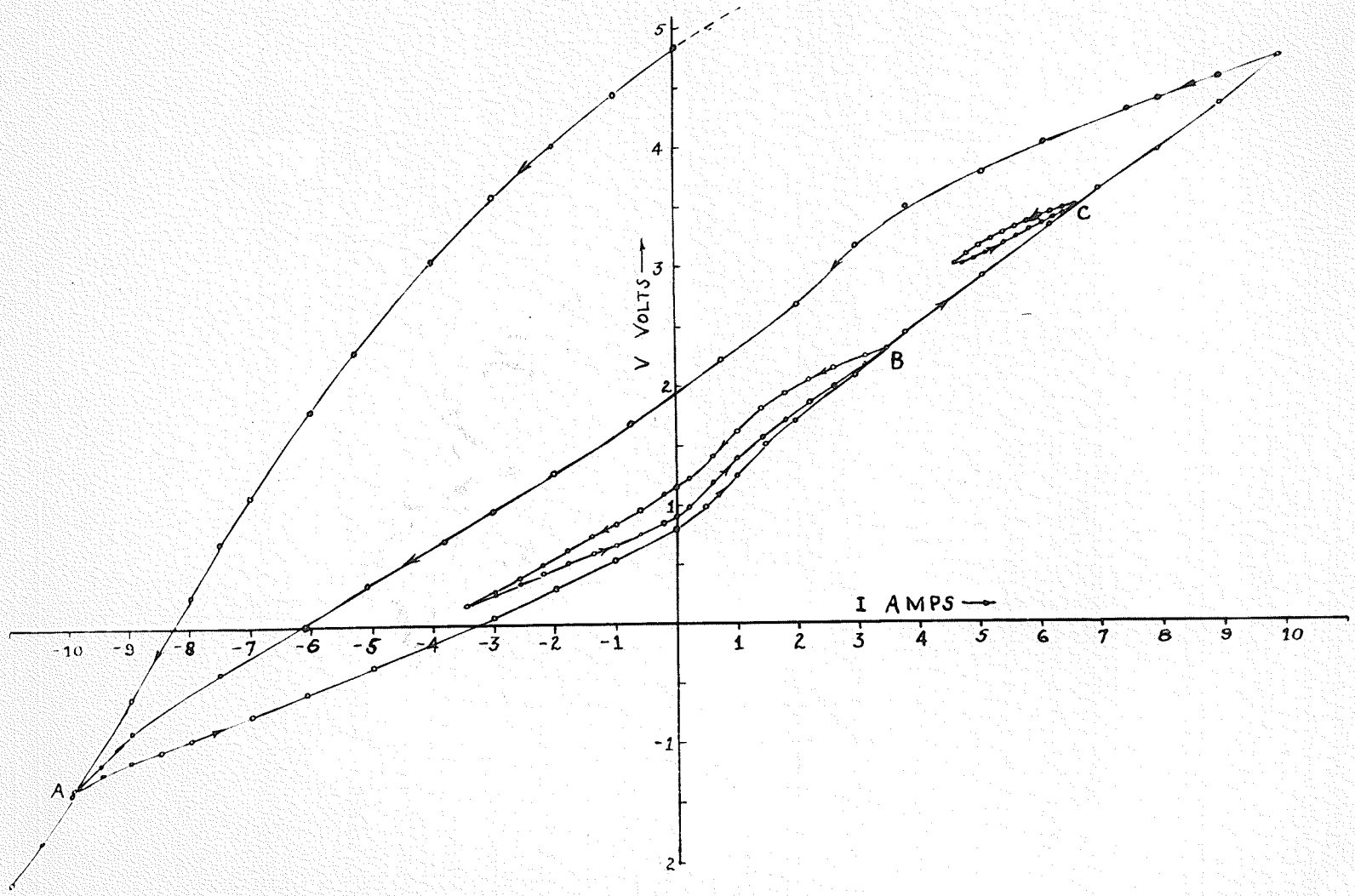

FIG XIV

CONCLUSIONS

In the majority of cases, especially where the half life of the beta activity is greater than one day, the beta spectra to be analyzed will be less than 1.5 Mev. The ideal auxiliary loop for analyzing such a spectrum is the 3.5 ampere loop described in the previous section. If, on this cycle, the current of - 3.5 amperes is increased to zero and then to + 3.5 amperes, the full spectrum of a 1.6 Mev particle will have been covered. When passing through a line where it is desirable to get as many points as possible, it is unnecessary that voltage readings be taken for every small increment of current. If the increments are .01 amperes, voltage readings need only be taken every ten settings since the curve can be taken as linear over distances of .1 amperes providing I is increased or decreased steadily in the same direction without backtracking. The application of this can be seen in the spectrum of Au^{198} appearing in Figure XV, where twenty points are taken in the .01 volt interval across the peak.

This curve was taken to calibrate the voltage scale of the field measuring device. Since the K line (e^- of 330.5 Kev) appearing at .540 volts requires an $H\rho$ of 2230 and ρ = 16 cms., then V must be multiplied by 4160 to find the corresponding $H\rho$, or 260 to find the corresponding field strength in oersteds. This checks with the L line (e^- of 396.6 Kev) appearing at .601 volts, and also with the

saturation field strength of 1260 oersteds at 5.83 volts.

It can thus be concluded that the magnet and field measuring device, although capable of giving points .1 oersted apart, can also give field strengths up to 1700 oersteds; properties which enable the unit to scan beta spectra in detail up to 7.5 Mev, and yet avoid completely the problems of stabilizing extremely large currents.

It seems likely that these valuable properties might eventually lead to the application of similar arrangements in certain other fields of work. Mass spectroscopy, electron microscopy, meson studies at high altitudes and nuclear resonance studies represent possibilities in this respect.

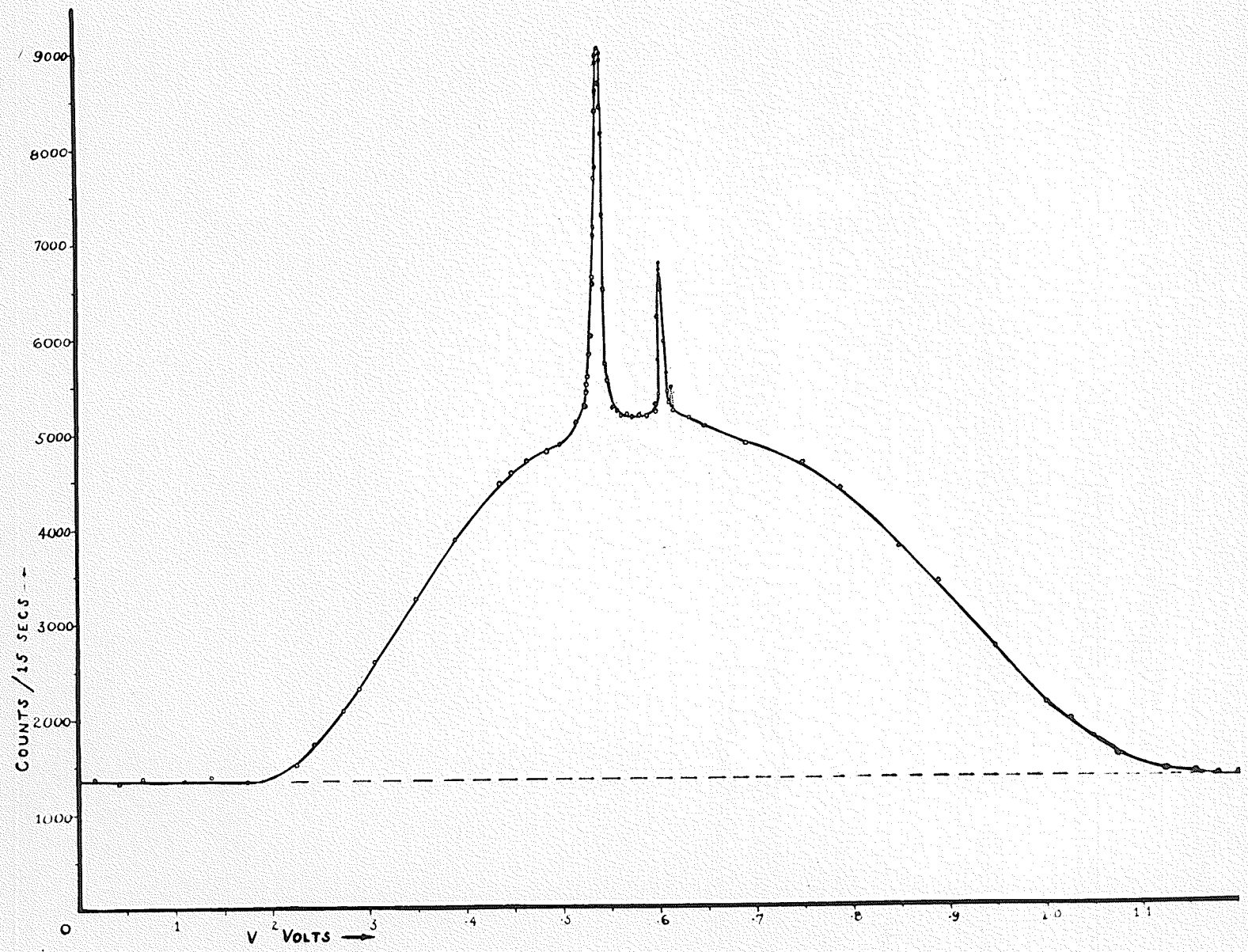
9000
8000
7000
6000
5000
4000
3000
2000
1000
COUNTS / 15 SECS →
0
1
2
3
4
5
6
7
8
9
1.0
1.1
V VOLTS →

FIG. XV

PART B

A NEW METHOD

OF

NEUTRON CAPTURE

GAMMA-RAY SPECTROSCOPY

INTRODUCTION

The theory of quantum mechanics tells us that systems may exist in quantized energy levels or in an energy continuum. In nuclear systems there is much evidence that quantized energy levels exist under certain conditions. However, since the nature of nuclear forces is not known as yet, nuclear wave functions which describe these levels cannot be computed from a Schroedinger-like equation for anything other than very special simple cases. Hence in studying nuclear levels, theory cannot guide experiment at this stage. These levels have been studied experimentally by determining the radioactive decay schemes in certain nuclei and in nuclear reactions that show capture and resonance effects.

The remainder of this paper will be devoted to the investigation of the possibility of obtaining energy level information on compound nuclei excited by the capture of a thermal neutron. This investigation of neutron capture gamma-ray spectroscopy has been attempted previously by other investigators (1),(2),(3), but in each case it was necessary to use the thermal neutron flux from a neutron reactor. In the present investigation only a weak 50 milligram Ra-Be neutron source is

---

(1) Bernard Hammermesh - Neutron Capture Gamma-Ray Spectra Phys. Review Vol.80. P.415 (1950)

(2) Richard Wilson - Neutron Capture Gamma-Rays from Cd, Cl and C - Phys. Review Vol.80. P.90 (1950)

(3) Kinsey, Bartholomew and Walker - Transitions to ground states in nuclei excited by slow neutron capture Phys. Review Vol.78. P481 (1950)

used and the spectrum is, for the first time, analyzed with the aid of a scintillation counter.

The following presentation follows a natural division into three parts. Consideration is first given to the neutron capture process with particular reference to neutrons of thermal energies. Neutron binding energies are considered and the most probable method of de-excitation of compound nuclei examined.

The second section is devoted first to the method of detection and then analysis of the gamma spectrum following neutron capture. The production of thermal neutrons, the experimental arrangement, processes involved in scintillation counting, and considerations of the resulting pulse height distribution constitute this section. The experimental method is then applied to the particular case of a Mn target and certain new results are presented.

THE NEUTRON CAPTURE PROCESS.

THE BOHR MODEL

To clarify the ideas of neutron capture we adopt the Bohr model of the nucleus. Under this concept, the nucleus consists of a densely packed system; with distances between nucleons of the same order of magnitude as the range of the nuclear forces, and interaction energies between nucleons of the same order of magnitude as the kinetic energies of the incident particles. Bohr argued that an incident particle hitting such a system would lose much of its kinetic energy in the first few collisions with the nucleons and would then be held by the nuclear forces. Thus he postulated as first step in any nuclear reaction, the amalgamation of target nucleus and incident particle into a compound nucleus. In this compound nucleus, the kinetic energy of the incident particle and the additional binding energy contributed by it are rapidly distributed among all the nucleons.

The second step of the reaction, the breaking up of the compound nucleus into the reaction products can take place only after a relatively long time because a large number of collisions is required before enough energy is likely to be "accidentally" concentrated on one nucleon to allow it to escape from the nuclear binding forces.

NUCLEAR RESONANCES.

The compound nucleus in its excited state corresponds to a particular energy level or quantum state above the ground state and as such has a certain mean life τ, i.e. the mean length of time before the system of its own accord passes to a state of lower energy. Each such state has a level width Γ which tells us how accurately the energy of the level can be measured. From Heisenberg's Uncertainty Principle we get

$$\Gamma \tau \approx \frac{h}{2\pi}$$

$$\text{or} \qquad \tau \approx 6 \times 10^{-15} \text{ seconds.}$$

if $\Gamma = .1$ ev as is the case in thermal neutron energy resonances. We can also use this principle to determine the time required for an incident thermal neutron to share its energy with the nucleus. If we suppose the neutron to have a binding energy of 8 Mev, then this will be the ΔE absorbed in amalgamating with the nucleus, and the Δt required will be

$$\Delta t \approx \frac{h}{2\pi \Delta E} = \frac{6.6 \times 10^{-27}}{2\pi (8 \times 1.6 \times 10^{-6})}$$

$$\approx 8 \times 10^{-23} \text{ SECONDS}$$

which is only 10^{-8} of τ, the mean life for the excited level. In this neutron absorption process, the newly created compound nucleus, being excited, will of course be metastable and will decay into a residual nucleus in its

ground state with the emission of some kind of radiation. This decay may in some cases take place in more than one stage.

The energy balance of the above processes is as follows: The original system is in the energy state $(E_{M_o} + E_n)$, E_{M_o} being the ground state level of the original nucleus and E_n part of the continuous spectrum of the incident neutrons. If the original nucleus is (A, Z) there will be in general some probability of forming the "compound nucleus" (A + 1, Z). However, this nucleus will possess certain discrete energy states and if $(E_{M_o} + E_n)$ does not lie near one of these levels, it is unlikely that the "compound nucleus" states will be excited. All that will happen is that the neutron will to some extent be reflected by the nuclear surface or "potentially scattered".

If on the other hand $E_{M_o} + E_n$ lies near a level of the compound nucleus, there will be a considerable probability of exciting those levels of the system corresponding to the existence of the compound nucleus.

Enquiring into the character of those levels of the "compound nucleus" which enter into the neutron capture problem, let the energy of the ground state of the compound nucleus be E_{C_o}. To decompose it into a neutron at rest plus initial nucleus takes an amount of work equal to the binding energy $(BE)_n$ of the neutron. Therefore the ground state of the compound nucleus lies a distance $(BE)_n$ below

that of the initial nucleus. The condition for resonance is then:

$$E_c^* = E_{c_o} + (BE)_n + E_n = E_{M_o} + E_n$$

E_c^* is an excited level of compound nucleus.

The level spacing will depend on the excitation of the compound nucleus, but will not vary greatly over small regions of energy. Hence for incident slow neutrons, the spacings of the resonances should show no marked changes in the narrow range of energies involved. Statistical analysis of thermal resonances in the neighbourhood of A = 100 indicate the mean level spacing for excitations equal to the neutron binding energy is of the order of 10 ev.(1)

For slow neutron processes only neutrons with orbital angular momentum zero can give rise to a compound nucleus. Thus the level spacing that must be considered is only that for states with angular momentum (spin) differing by one half from that of the initial nucleus.

The cross section for resonance capture of a neutron of energy E_n in a target nucleus ${}_zM^A$ followed by emission of a particle b is given by the Breit-Wigner theory (2),(3)

---

(1) Bethe; Review of Modern Physics, vol.9. P.79 (1937)
(2) G. Breit, E. Wigner; Phys. Review Vol.49. P.519 (1936)
(3) E. P. Wigner; Phys. Review Vol.70. P.606 (1946)

and is: $$\sigma_{nb} = \frac{\lambda_n^2}{4\pi} \frac{\Gamma_n \Gamma_b}{(E_n - E_0)^2 + \frac{1}{4}\Gamma^2} \quad - - - - - - (A)$$

where λ_n = wavelength of incident particle (neutron)

Γ = total level width

Γ_n = partial level width for neutrons

Γ_b = partial level width for emission of particle b

E_0 = energy of neutron at resonance.

This equation applies to the case where head-on collision is assumed and any effects due to the spin of the particles involved are neglected.

MODE OF DECAY

We consider a particular transition involving emission of a particle b leaving the residual nucleus in a given energy state E_b. The state of the residual nucleus is defined completely by the state of the particle. By standard perturbation theory the probability per unit time of this process is

$$\frac{1}{\tau_b} = \frac{2\pi}{\hbar} |H|^2 \rho_b(E_b)$$

where H is the "matrix element" of the transition and ρ_b is the density of states available to the emitted particle of energy E_b. Putting $\Gamma_b = \hbar/2\pi\tau_b$ we have: $\Gamma_b = 2\pi |H|^2 \rho_b$ The density of states ρ_b presents itself in this formula because the process of derivation involves box quantization in which we consider emission as being into a volume Ω.

The density of states in momentum space is by Statistical Mechanics $\frac{\Omega}{h^3}$. The number of states with momentum p to p + dp is

$$\frac{\Omega}{h^3} \cdot 4\pi p^2 \, d(p)$$

but by definition this is:

$$\rho_b(E)\, d(E) = \frac{\Omega}{h^3} \cdot 4\pi p^2 d(p)$$

For particles $E = p^2/2m$ so $\frac{d(E)}{d(p)} = v$

and for photons $\frac{d(E)}{d(p)} = c$

Thus: for particles $\rho(E) = \frac{4\pi\Omega}{h^3} \frac{p^2}{v} = \frac{4\pi\Omega}{h^3} \sqrt{2m^3}\, E^{1/2}$

for photons $\rho(E) = \frac{4\pi\Omega}{hc^3} v^2$

Here we see one reason why, for low energies of incoming neutrons, decay of the compound nucleus by gamma emission is much more likely than re-emission of a neutron; for the probability of neutron emission approaches zero with the velocity of the incident neutron. For gamma-rays on the other hand, the frequency of emitted quanta depends on the next lower level of the compound nucleus into which it is permitted by the selection rules to radiate. This sets a lower limit to the frequency ν and hence to $\rho(E)$ however small the neutron energy.

THERMAL NEUTRON CROSS SECTIONS.

Suppose the resonance level considered is the first above $E_{c_o} = o$ at say E_o. If we extend the range of incident neutron energies down to $E_{c_o} = o$ subject only to

$E_n << E_o$ it is found that a compound nucleus can still be formed and decay by different processes each having a different mean life (τ).

Assuming the probability for emission of b is constant with energy over this range, that is Γ_b = constant, we must assume $\Gamma_n = kv$ where k is a constant and v is velocity of neutron.

This assumption follows from the fact that emission of n with a certain momentum varies as the density of states in momentum space at that momentum.

$$\text{i.e.} \qquad \propto \; 4\pi p^2 \frac{d(p)}{d(E)}$$

$$\propto \; p$$

Assuming $\Gamma_n = kv$ then Eqn (A) page 7, becomes:

$$\sigma_{nb} = \frac{\Gamma^2 \sigma_o \left(\frac{E_o}{E_n}\right)^{1/2}}{\Gamma^2 + 4(E_n - E_o)^2} \qquad ----- (B)$$

taking $1/\lambda_n^2 \propto E_n$ and σ_o cross section at resonance.

For $E_n << E_o$ as will be the case for thermal neutrons ($E_n \approx \frac{1}{40}$ ev)

(B) becomes:

$$\sigma_{nb} = \frac{k}{\sqrt{E_n}} = \frac{k'}{v_n}$$

which is the familiar $\frac{1}{v}$ law for neutron capture processes.

Hence for the case of incident neutrons of thermal energies ($\frac{1}{40}$ ev) where v is very small, there will be a fairly large cross section and as seen in the previous section the predominant reaction will be (n γ).

EXPERIMENTAL ARRANGEMENT AND ANALYSIS OF NEUTRON CAPTURE GAMMA RAYS.

DETECTION OF NEUTRON CAPTURE GAMMA-RAYS.

The technique which we have employed in detecting neutron capture gamma-rays can most readily be understood by referring to Figure XVI.

Fast neutrons from the 50 mc. Ra-Be source are slowed down to thermal energies by elastic collisions in the paraffin block. This thermal neutron flux strikes the target surrounding the crystal phosphor (Na I - Tl). Upon capturing a neutron, the target nucleus emits gamma radiations. Some of these gamma-rays strike the crystal phosphor, giving up some or all of their energy to an electron through photo-electric effect, Compton collisions, or pair production. The high energy electrons thus formed in the crystal excite fluorescent centres in the lattice producing bright flashes which might consist of several tens of thousands of photons. These photons are converted by the photo-multiplier into voltage pulses proportional to the light flash. These voltage pulses when suitably amplified can be analyzed according to energy either by photographing the pulses on a C.R.O. screen, or by pulse height sorting with a differential pulse discriminator and scaler.

The remainder of this section will first be devoted

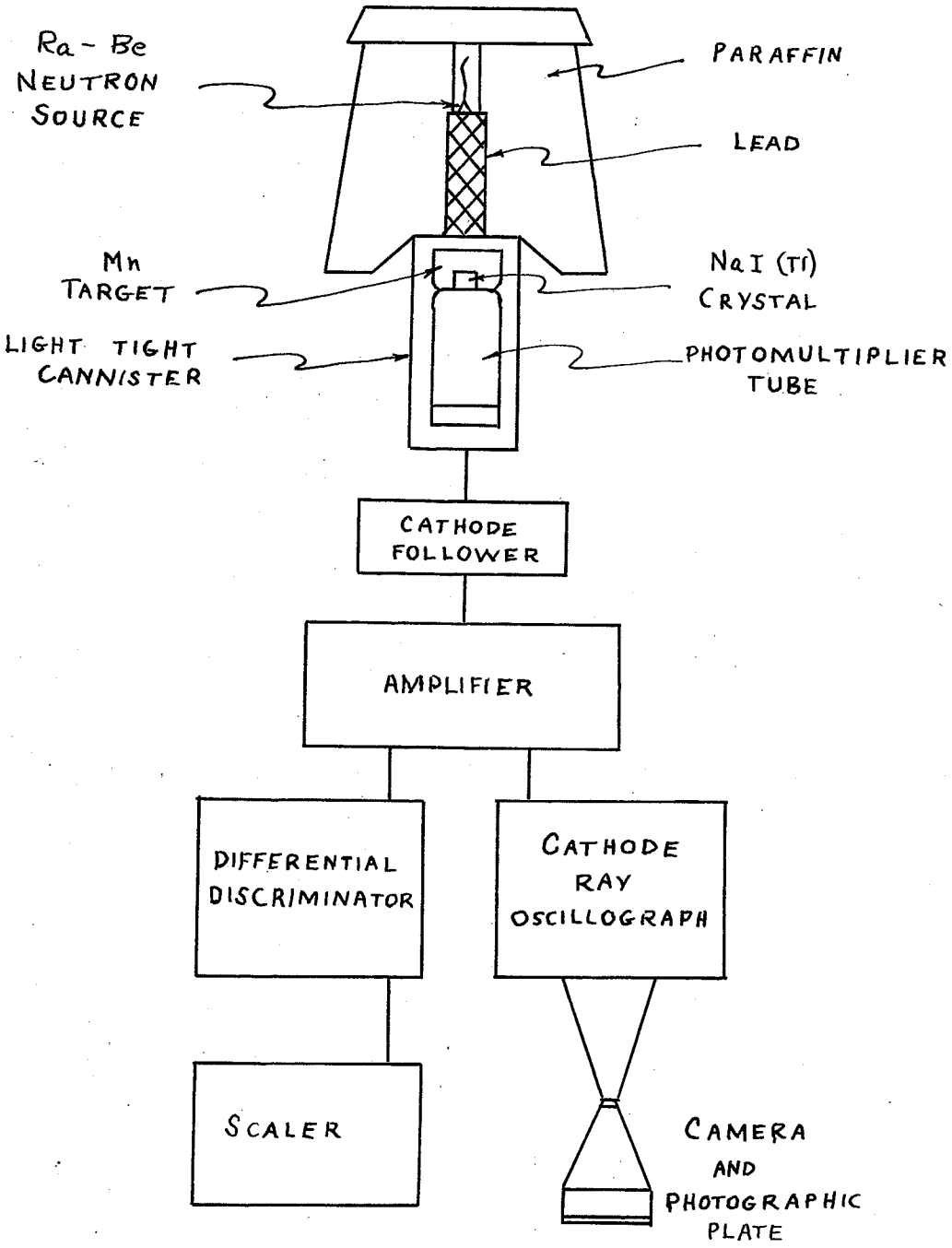
Ra - Be
NEUTRON
SOURCE
PARAFFIN
LEAD
Mn
TARGET
NaI (Tl)
CRYSTAL
LIGHT TIGHT
CANNISTER
PHOTOMULTIPLIER
TUBE
CATHODE
FOLLOWER
AMPLIFIER
DIFFERENTIAL
DISCRIMINATOR
CATHODE
RAY
OSCILLOGRAPH
SCALER
CAMERA
AND
PHOTOGRAPHIC
PLATE

FIG XVI

to description and consideration of the components of this detecting device and then to analysis of the resulting spectra.

THE NEUTRON SOURCE.

The neutron source employed was a 50 milli-curie Ra-Be[(1)] source. The neutrons in such a source are produced by the dual reaction

$$Be^9 + \alpha \rightarrow C^{12} + n + 5.5 \text{ Mev.}$$

$$Be^9 + \alpha \rightarrow 3\,He^4 + n \qquad \text{(feeble)}$$

Radium and its decay products are the alpha particle source; the radium and beryllium (ratio 1 to 5) being finely divided and well mixed because of the short range of alpha particles in solids. The source mixture is carefully sealed to prevent the escape of Radon.

The neutrons from this source are not mono-energetic for several reasons.

(1) The two different reactions involve different energies.

(2) The incident alpha particles are not mono-energetic. First, there are several different initial energies, and second, the particles may lose energy by collision before being captured by the beryllium.

(3) In any alpha capture process there is a complete distribution of angles between the incoming alpha

---

(1) Ra-Be neutron source rented from Eldorado Mining & Smelting Co.

particle and the outgoing neutron.

(4) The C^{12} nucleus can be left in an excited state.

Thus the Energy spectrum of neutrons extends up to 12 Mev. and has a most probable energy of 5 Mev.

An output of 3.4×10^5 neutrons/ sec. has been reported for a similar source (1).

Neutrons are thermalized in the hydrogenous material (paraffin) by elastic collisions with protons. A 2 Mev. neutron requires 25 collisions to reduce it to thermal energies (.025 ev).

Four inches of lead are used to reduce the direct effect of the Ra gamma-rays on the crystal.

THE CRYSTAL PHOSPHOR

For a crystal to be suitable for this purpose, it must produce radiations of extremely short duration in the spectral range to which the photo-electric device is sensitive, and must be reasonably transparent to this radiation, and must be efficient in converting the energy of the particle into visible radiation.

Every phosphor has a characteristic delay time, that is it continues to emit photons for a certain time after it has been struck by the incoming particle. If the mean decay time of a phosphor is 5 microseconds, the duration of the output pulse will be of this order. In the case of

---

(1) Gammertsfelder & M. Goldhaber. Phys. Review Vol.69. P.368 (1946)

Na I (Tl) this delay time is of the order of one half of one microsecond[1]. This is several times larger than the delay time of Anthracene, but the conversion efficiency of Na I (Tl) is much better than Anthracene. It is estimated that Na I (Tl) will produce 1000[2],[3] photo-electrons per Mev. of incident radiation from the cathode of a Photo-Multiplier tube while Anthracene produces less than one quarter of this. A good Na I (Tl) crystal will produce as many as 20,000 [4] photons of visible light in converting a 1 Mev. electron energy. This light is in the wavelength band of 4000 A° in which the self absorption of the crystal is very low, so a large crystal providing it is optically clear, may be used if it is desired. This spectral range is the same as that in which the cathode surface of the multiplier is sensitive.

The crystal Na I (Tl) has one serious disadvantage and that is its hygroscopic properties. However, coating the crystal in mineral oil prevents water vapor from attacking and clouding the surface, and also forms a light bond between the polished face of the crystal and the face of the photo-multiplier. In use, the top and sides of the crystal are

---

(1) Hofstadter, I.R.E. & A.I.I. Instrument Conference, Nucleonics Vol.4, No.2, P.51.

(2) J. A. McIntyre and R. Hofstadter, Phys. Rev. Vol.78. P.617 (1950)

(3) R. W. Pringle and S. Standill, Phys. Rev. Vol.80, P.762 (1950)

(4) G. A. Morton & J. W. Robinson - A Coincidence Scintillation Counter. Nucleonics, Vol.4, No.2, P.25 (1949)

wrapped in aluminum foil to increase light collection in the photo-multiplier, and this also serves as a protection.

THE PHOTO-MULTIPLIER

The photo-multiplier tube (British E.M.I. 5311) consists essentially of a 1" diameter semi-transparent photo sensitive cathode near the end window of the tube, followed by ten dynodes to the collector. The cathode has a response maximum at 4000 A° and a quantum efficiency of 6% at this value. Each of the dynodes consist of a material (Be-Cu) with a high secondary emission ratio (approximately four) and is arranged so that the secondary electrons emitted are electrostatically focussed on to the succeeding dynode when a suitable potential difference is applied. Operated at a voltage of 100 volts per stage the gain of this multiplier is approximately 1×10^{6}. Hence one photo-electron released at the photo-cathode will represent a charge of 1.6×10^{-13} coulombs at the collector. Since the capacitance of collector and associated circuit is limited to 10 $\mu\mu$f. the voltage pulse produced by one photo-electron is 15 millivolts. The output pulse must be fed through a cable to the amplifier so it is necessary that it be first fed into a cathode follower circuit which acts as a low impedance source. This modification was built around the base of the tube which was then enclosed in a light tight cannister as shown in figure XVI. The voltage between stages was controlled by a precision voltage divider in parallel

with a 2000 volt D.C. supply regulated to within .1%, and the potential of the individual electrodes established by voltage drops across a chain of ten 1.6 megohm resistances in parallel with the divider.

THE DIFFERENTIAL PULSE HEIGHT ANALYZER.

The pulses coming from the cathode follower at the photo-multiplier were fed into a linear amplifier (Atomic Instrument Company, Model 204-C, Serial number 249) and then had to be analyzed.

The pulse height analyzer is described in an earlier paper[1]. It comprises two modified Schmitt trigger circuits feeding into an anti-coincidence unit, where only pulses lying between two pre-set trigger levels produce output pulses.

This enables the pulse height distribution coming from the amplifier to be scanned in detail in either one or two volt "gates" (difference in the two trigger levels), as desired. The pulses are counted on a scaler (Atomic Instrument Company, scale of 1000, model 105), and the results for any given investigation plotted as a No. of counts v.s. Pulse height in volts distribution.

The advantage of the differential method of scanning pulse height distributions, compared with the former

---

(1) K. I. Roulston, A Simple Differential Pulse-Height Analyzer, Nucleonics Vol.7, No.4, P.27 (1950)

method of integral counting above pre-set discriminator levels followed by subtraction to find the number of pulses lying within the desired trigger levels, is considerable. In the integral counting method, the probable error in the number of counts between two trigger levels (say $N_1 - N_2$ where N_1 is the number of counts above one level and N_2 the number above a second level), is approximately $.67 \sqrt{N_1 + N_2}$ whereas in the differential method the error is approximately $.67 \sqrt{N_1 - N_2}$. Hence the fractional error, obtained when the probable error is divided by the number of counts in the interval $(N_1 - N_2)$, is considerably greater in the former case than in the latter.

CATHODE RAY OSCILLOGRAPH

PULSE-HEIGHT ANALYZER

In Figure XVI it will be seen that alternative methods are illustrated in analyzing the pulse-height distribution from the amplifier. In the second case, the pulses are all displayed on the screen of the oscilloscope (Tetronix Inc. Model 511A) and proper amplification, or attenuation introduced to obtain the largest trace pattern without blocking. In this case the height of the pulse on the screen is proportional to the pulse voltage, and if a photograph is taken of a spectrum over a period of time, the integrated blackening on the negative gives a direct indication of the number of pulses within any given voltage range. Examples of such spectra appear in

Figures XVIII and XIX and will be explained in detail in the next section.

To obtain clear line spectra it was necessary to stabilize the power input of the oscilloscope, and use a medium fast ortho film which minimized the "aura effect" on the scope screen due to light from the filament. A simple method of putting a base line on the photograph without disturbing the camera was devised and energy measurements could then be made between the pulse height peaks and the base line. Energy measurements made in this way by projecting the negative on to a screen, correlated exactly in most cases to ratios determined with the differential discriminator, the former having a better resolution than the latter.

ANALYSIS OF SPECTRA.

Gamma-rays interact with matter by the three well known processes of photo-electric effect, Compton effect and pair production. In the sodium iodide crystal, the method by which an incident gamma-ray will impart its energy to an electron depends upon the energy of the gamma ray(1). Since iodine forms 85% by weight of the Na I (Tl) crystal we may consider how the cross sections for these

---

(1) For a description and complete bibliography of earlier work see R. W. Pringle Nature Vol.166, P.11, 1950.

different processes vary with energy in Iodine to get an indication of what to expect for any given energy gamma radiation. This information appears in Figure XVII in the form of cross section for the different effects against energy.

It will be expected that the photo-electric effect would produce strong lines for energies up to 2 Mev. These lines will appear with the full energy of the incident radiation, since in the majority of cases subsequent X rays following K or L electron removal will be captured. Above 2 Mev. the pair formation process becomes increasingly significant. These lines will appear with the incident gamma radiation energy, minus 1.02 Mev, corresponding to the $2\ m_o\ c^2$ of electron-positron pair formation. Capture of one of the annihilation quanta will produce pulses .51 Mev. farther on and capture of both annihilation quanta will produce a very small peak at the full energy.

The Compton effect has a large cross-section over the lower energy region and falls off toward higher energies where pair formation is dominant. This effect does not tend to produce as sharp a line as the other two effects (which eventually produce gaussian distributions due to the statistical fluctuations within the photo-multiplier). However at energies where the effect is prominent the effect does have a characteristic shape. It is fairly sharp on the high energy side but falls off gradually on the low energy side.

The difference in the distribution due to these two effects is shown in Figure XVIII which is an application of the photographic technique to the spectrum of Co^{60} The two lines at the top A and B correspond to photo-electric lines of gamma-ray energies of 1.17 Mev. and 1.33 Mev. These lines are superimposed on the Compton distribution of both which has a peak below these two lines at C.

It is possible to analyze a more complex spectrum in this energy range by comparison. The gamma spectrum of radium appears beside a cobalt distribution in Figure XIX. The lines D E F and G correspond to photo-electric lines at energies of 1.75 Mev, 1.40 Mev, 1.10 Mev. and .610 Mev.(1) The Compton peak of the 1.10 Mev. radiation appears between F and G and for the 1.40 Mev. and 1.75 Mev. radiations causes a slight spreading of the lines E and F. Longer exposures on this spectrum bring out the photo line of 2.2 Mev. and 2.45 Mev, as well as the pair line at 1.2 Mev. due to the 2.2 Mev. gamma radiation.

Figure XX illustrates the spectrum of a Po-Be source. The high energy line corresponds to the pair line at 3.45 Mev. belonging to the gamma radiation of 4.45 Mev. following de-excitation of the C^{12} nucleus formed in this source. The faint line appearing above this corresponds to capture of a single annihilation quanta. The low energy spectrum

---

(1) Rutherford, Chadwick and Ellis, Radiations from Radio-active Substances, Cambridge Univ. Press.

corresponds to radium contamination in the source giving lines at the energies discussed previously and in addition the low energy photo line at .77[1] Mev. due to a polonium nuclear gamma-ray.

---

(1) Zajac, Broda and Feather - a Further study of Gamma Radiation from Po: Proc. Phys. Soc. Vol.15 P.501 (1948).

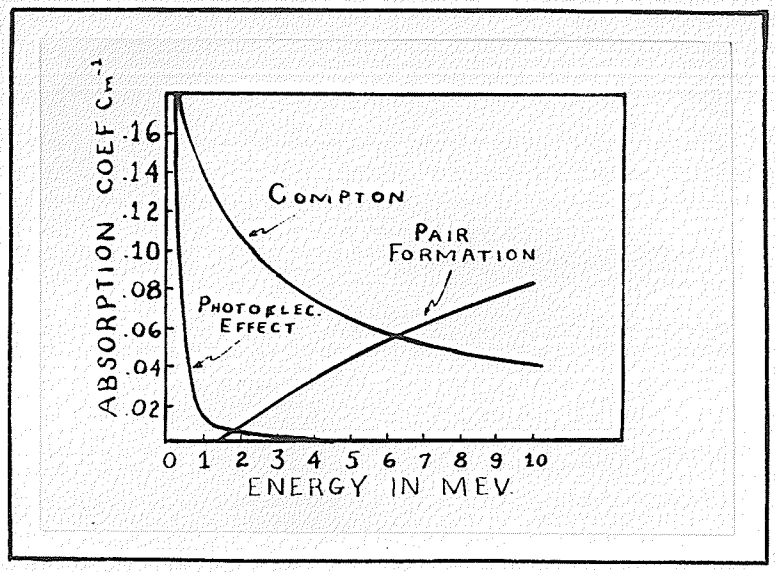

FIG. XVII

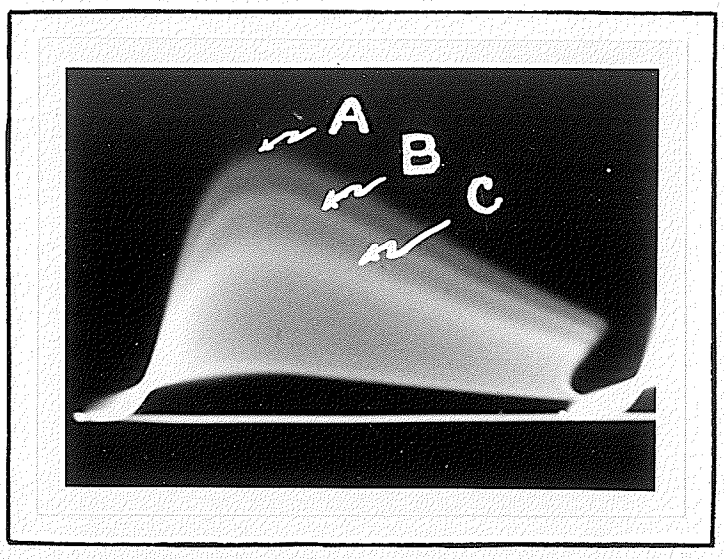

FIG. XVIII

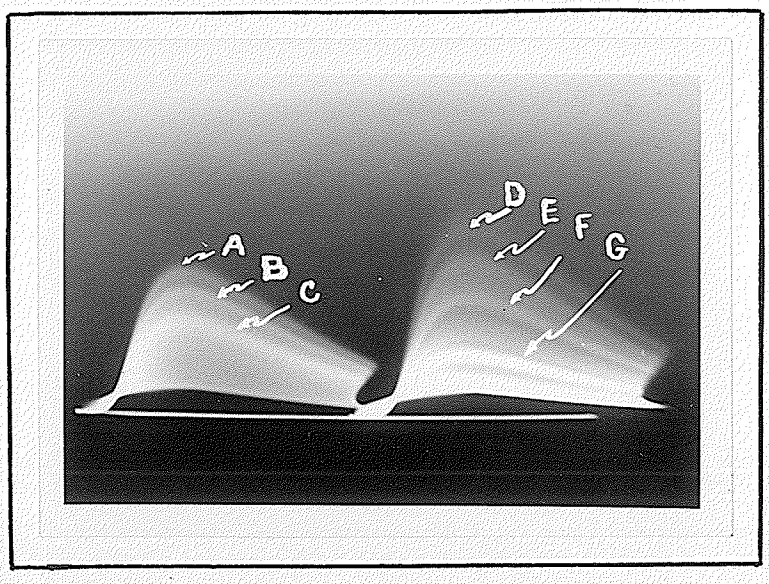

FIG. XIX

ANALYSIS OF THE Mn ($n\gamma$) SPECTRUM

To obtain the Manganese neutron capture gamma spectrum the apparatus was set up as indicated in Figure XVI. A Na I (Tl) crystal cylinder about 1.5 cms. in diameter and 1.3 cm. high was polished, coated in mineral oil and placed on the photo-multiplier end window. About 40 gms. of metallic manganese was then placed on top and around the crystal on top of the photo-multiplier. The cannister was then closed and taped to ensure the system was light tight, the paraffin block placed on top of the can as shown and the Ra-Be source placed above the lead plug. A voltage of 570 volts was applied across the ten dynodes and collector of the E.M.I.5311 giving a potential drop of approximately 50 - 60 volts per stage.

Using the differential discriminator the resulting spectrum was scanned in one volt steps and plotted. Simultaneous with this, a photograph of the spectrum was taken on the oscilloscope. To calibrate the resulting energy spectrum the Po-Be source was then located on top of the crystal and the pair line at 3.43 Mev. of the 4.45 C^{12} radiation located by scanning its spectrum.

Removing both the Po-Be and the Mn. from around the crystal, a background run was taken. The true Mn ($n\gamma$) spectrum with this background subtracted appears in Figure XXII. The shape and energy distribution of this curve was found to be consistant on several such runs.

Assuming an energy of 4.45 Mev. for the calibration peak appearing at A, two definite pair lines can be identified at B and C in the Mn. neutron capture spectrum. These correspond to electron energies of 4.35 Mev. and 6.13 Mev. or gamma radiations of 5.37 and 7.15 Mev. The higher energy presumably corresponds to the ground state transition in the Mn^{56} and is equal to the binding energy of the last neutron, while the lower value indicates a level in Mn^{56} at 7.15 - 5.37 or at approximately 1.78 Mev. The intensities of these two lines are approximately equal. Transitions from this state to ground could not be analyzed because of the high background.

The assumed value of 4.45 Mev. for the Po-Be line is fairly reliable. Bradford and Bennett[1] report the line at 4.44 or 4.46 based upon the measurement of the neutrons produced by mono-energetic alpha particles. Pringle, Roulston and Standil[2] reported a value of 4.40 ± .05 last year, but recent refinements have raised this value to 4.45. Bell and Jordan[3] also using a scintillation pair spectrometer assess a value of 4.44 ± .03 Mev. This value is also consistent with the known values of the radium lines appearing in the photographed

---

(1) Bradford & Bennett: Phys. Rev. Vol.78, P.302, (1950)
(2) Pringle, Roulston & Standil: The Gamma-Rays from Be Phys. Rev. Vol.78, P.627 (1950)
(3) Bell & Jordan: Gamma-Rays from Po-Be Neutron Source and the excited state of C Phys. Rev. Vol.79, P.392 (1950)

Po-Be spectrum Figure XX. The energies given for this line are tabulated below:

Bradford and Bennett	4.44 4.46	Probable Value 4.45 ± .02 Mev.
Pringle, Roulston & Standil	4.40 ± .05	
Re-assessed Value Pringle, Roulston & Standil	4.45 ± .03	
Bell & Jordan	4.44 ± .03	

Estimations of the energy of these lines could also be made from the photographs. A typical photographed spectrum of Mn^{55} (nγ) appears in Figure XXI. Energy calibrations were done by photographing the Mn (nγ) spectrum and Po-Be spectrum simultaneously, and also consecutively. Ratio measurements were then taken from the common base line and the energies of the lines calculated. The results appear in tabular form below:

Photograph Average	7.17 Mev, 5.27 Mev.
Discriminator Run Average	7.15 Mev, 5.37 Mev.

Allowing for the possible calibration error, it can be claimed that these two gamma radiations are 7.16 ± .05 Mev. and 5.32 ± .05 Mev. This final set of values indicates the level in Mn^{56}, referred to above, to be at 1.84 Mev.

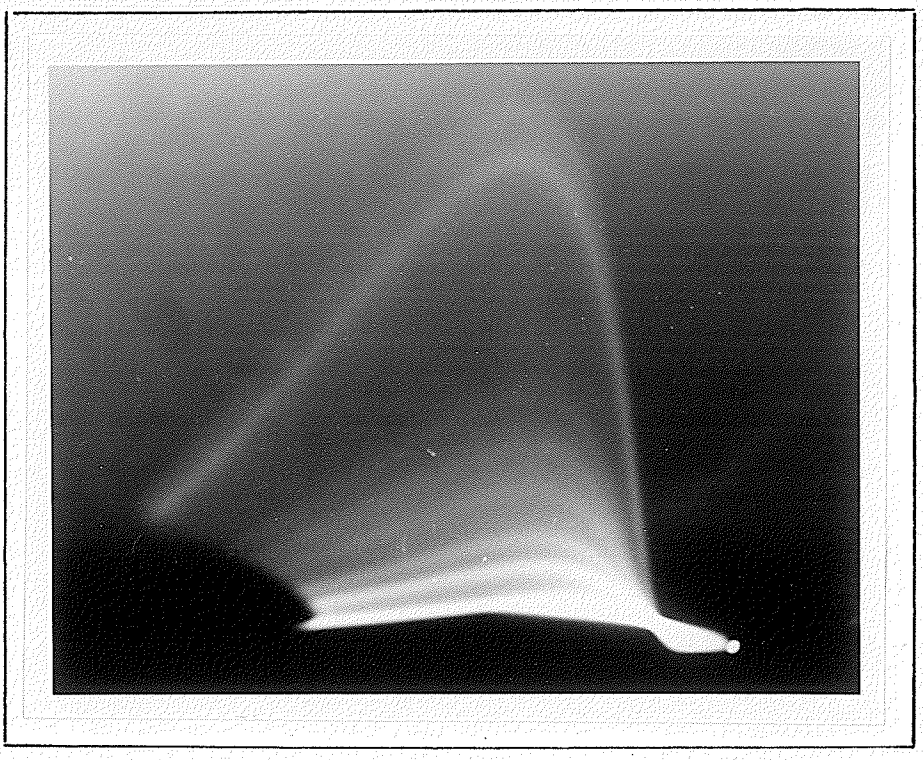

FIG. XX

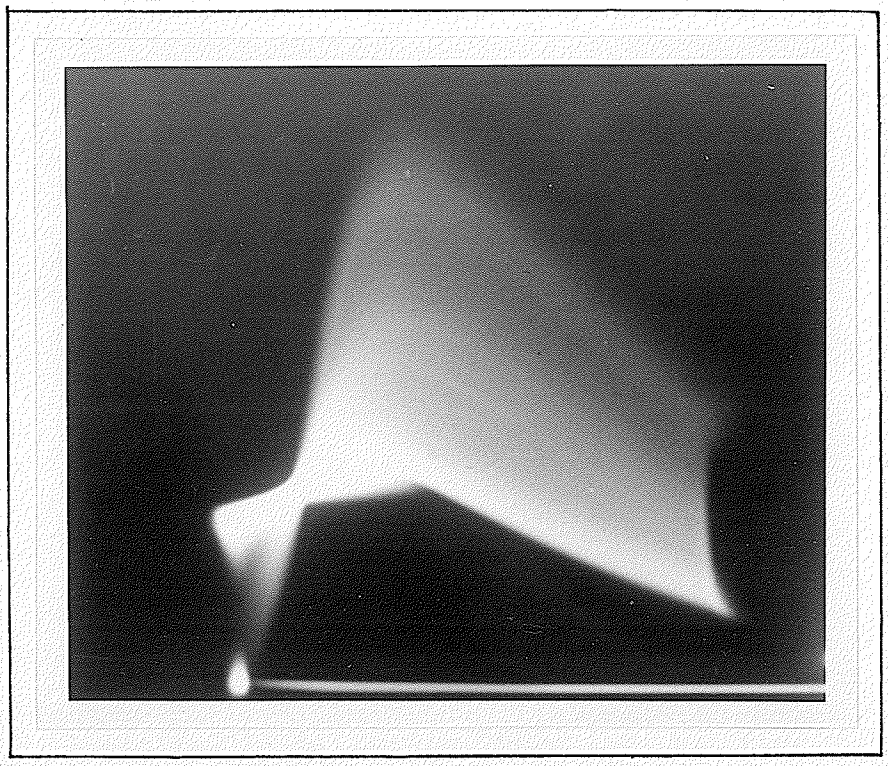

FIG. XXI

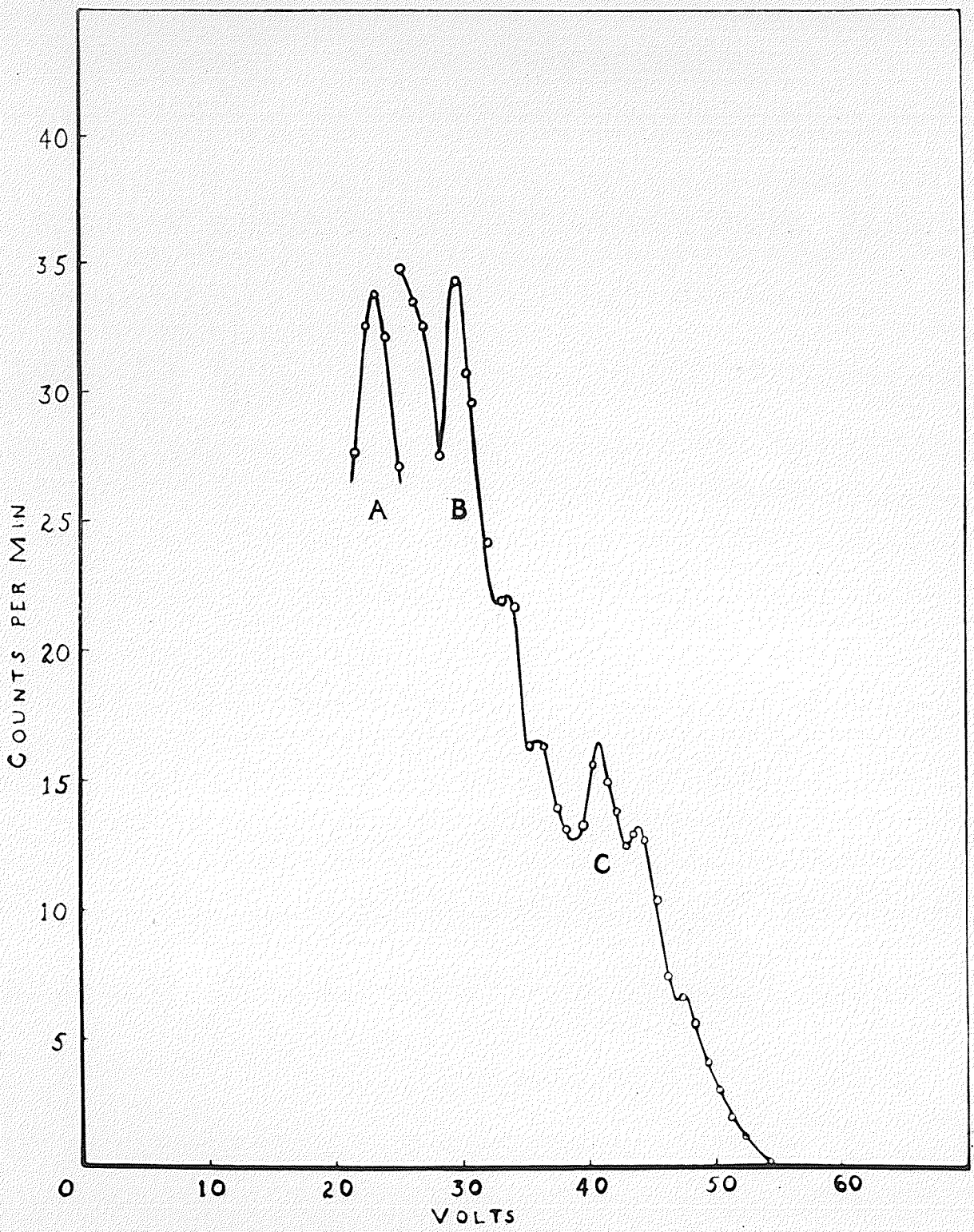

FIG XXII

CONCLUSIONS.

It can be concluded that it is possible to investigate ($n\gamma$) spectra for elements using a relatively weak thermal neutron source because of the extreme sensitivity of the scintillation counting device. Although only the results for Mn^{55} ($n\gamma$) are included in this paper, investigations of Cl, Cd, and even Pb have been made with favorable results. It is very interesting to note that the detecting device remains linear up to such high energies. This last feature was found to be true only when the voltage between stages was lowered considerably. Evidently if the gain in the multiplier is too large, the pulses produced by these extreme energy particles saturate the system and produce a gradual non-linearity rather than a blocking effect or pile up at the end.

The value 7.16 ± .05 Mev. for the binding energy of the neutron in Mn^{56} is just compatible with the only published value of 7.25 ± .03 obtained very recently by Kinsey, Bartholomew and Walker[1] using the intense neutron flux from the Chalk River pile and analyzing the spectrum with a magnetic pair spectrometer. This method gives a resolution of two percent.

Kinsey et al do not report any evidence for the

---

[1] Kinsey, Bartholomew and Walker - Transitions to the ground states in Nuclei excited by Slow Neutron Capture. Phys. Review Vol.78, P.481, (1950)

5.32 Mev. gamma-ray and so no earlier determinations have been published on the level appearing in the Mn^{56} at 1.84 Mev. Since Mn^{56} is not the decay product of any known isotope, it is not yet possible to obtain independent evidence on this level. The resolution of pair lines by this method is approximately 7%, using the differential discriminator, but close to 3% if use is made of the photographic technique, showing that the former method has caused considerable broadening of the pair lines.

ACKNOWLEDGEMENTS.

The writer wishes to express his sincere thanks to Dr. R. W. Pringle for his constant interest and direction; to Prof. K. I. Roulston for advice on the use and adjustments to the differential discriminator; to S. Standil for advice and assistance in the operation of the beta spectrometer used in calibration of the magnetic field, and to Mr. S. Bird for advice and technical assistance in the construction of field measuring devices.